UNSTEADY FLOW NEAR A CIRCULAR CYLINDER OSCILLATING IN LINE WITH AN INCIDENT UNIFORM FLOW

Vinícius Borges de Oliveira, vinicius.b.oliveira@hotmail.com
Luiz Antonio Alcântara Pereira, luizantp@unifei.edu.br
Institute of Mechanical Engineering, Federal University of Itajuba, Itajuba, Minas Gerais, Brazil, CP 50

Miguel Hiroo Hirata, hirata@superonda.com.br
State University of Rio de Janeiro, FAT-UERJ, Resende, Rio de Janeiro, Brazil

Abstract. *This paper describes the vorticity shedding from a circular cylinder oscillating in the direction of an incident uniform flow. We use a cloud of discrete vortices to investigate numerically the influence of cylinder oscillation frequency on the lock-in phenomenon of Kármán vortex shedding. The aerodynamic loads are computed using an integral formulation derived from the pressure Poisson equation. Results are examined for Reynolds number of around 100,000 and a large oscillation amplitude. Our results indicate several types of vortex shedding mode.*

Keywords*: vortex method, circular cylinder, in-line oscillation, lock-in, aerodynamic forces*

1. INTRODUCTION

In scientific terms, the flow around cylindrical bodies includes a variety of fluid dynamics phenomena, such as separation, vortex shedding and the transition to turbulence. The mechanisms of vortex shedding and its suppression have significant effects on the various fluid-mechanical properties of practical interest: flow-induced forces, vibrations and noises and the efficiencies of heat and mass transfer, for example. For a better and easy understanding of the physics, therefore, it is reasonable to focus our attention on the flow around bodies of simple geometry such as a circular cylinder.

Cylinders having a two-dimensional structure are very suitable for restricting the complexity and thus observing the fundamental features of the flow. One of the most interesting features of this flow is the phenomenon of synchronization, in which the frequency of vortex shedding, f, coincides with that of the cylinder oscillation, f_b; this is also known as "lock-in". The literature is plenty of materials on the subject and previous works have reported that the lock-in features and vortex shedding patterns in the flow around an in-line oscillating cylinder differ significantly with those in flows around a stationary cylinder or a cylinder oscillating transversely. For instance, vortex shedding frequency f had been found to lock-in to the forcing frequency f_b when f_b is close to the free vortex shedding frequency f_{so} in the transverse oscillating case. But, the in-line vibration lock-in takes place at a number of multiple ratios of f_b/f_{so}, especially, at f_b/f_{so} =2.0, where the lift and drag forces increase greatly. Comprehensive reviews can be found in Koopman (1967), Sarpkaya (1979), Bearman (1984), Blevins (1990), Griffin and Hall (1991), Williamson and Govardhan (2004) and Hirata *et al.* (2008).

Koopman (1967) investigated the lock-in region in terms of the oscillation amplitude A and the frequency of a circular cylinder f_b. He showed that the Kármán vortex is more likely to lock-in when f_b is closer to the vortex shedding frequency from the fixed cylinder, f, i.e. the threshold amplitude is lower when f/f_b is closer to unity. He also reported that there exists a definite value of oscillation amplitude below which the lock-in does not occurs even when f/f_b=1.

The experimental work of Williamson and Roshko (1988) deals with the synchronization regions and identifies many modes and vortex wake patterns with detailed explanations and descriptions; due to the difficulties in the experimental visualizations the Reynolds number were kept below 600.

The numerical work of Hirata *et al.* (2008) simulated the flow around a heaving circular cylinder by using vortex method. Their results showed that there are three characteristic bands for the body oscillating frequency. Band I, for which $f_b \rightarrow 0$, the body oscillation has little influence and the vortex shedding frequency is almost independent of the body oscillating frequency. Band II represents a transition band in which the lock-in is partial and one can identify simulation periods in which lock-in is observed followed by simulation periods where this does not occurs. Finally in the uppermost Band III the inertial components dominate the lock-in is always observed. The numerical findings show that the lock-in frequency depends on the amplitude of the body oscillation; in fact it decreases linearly with it in accordance of the low Reynolds number findings of Williamson and Roshko (1988).

This paper utilizes the vortex method code developed by Hirata *et al.* (2008) to simulate numerically the vortex shedding from an in-line oscillating circular cylinder in a uniform flow. In this study, the focus is upon lock-in of the Kármán vortex caused by a higher-amplitude cylinder oscillation. The transition behavior from non lock-in to lock-in is investigated by using two reference frames; the body fixed frame oscillates with respect to the inertial frame of reference. A cloud of free vortices is used in order to simulate the vorticity, which is generated on the body surface and develops into the boundary layer and the viscous wake. Each individual free vortex of the cloud is followed during the numerical simulation in a typical Lagrangian scheme. Important features of the vortex methods (Chorin, 1973; Leonard,

1980; Sarpkaya, 1989; Sethian, 1991; Lewis, 1999; Alcântara Pereira *et al.*, 2004; Kamemoto, 2004; Stock, 2007) are: (i) it is a numerical technique suitable for the solution of convection/diffusion type equations like the Navier-Stokes ones; (ii) it is a suitable technique for direct simulation and large-eddy simulation; (iii) it is a mesh free technique; the vorticity field is represented by a cloud of discrete free vortices that move with the fluid velocity.

Vortex cloud simulation offers a number of advantages over the more traditional Eulerian schemes for the analysis of the external flow that develops in a large domain; the main reasons are: (i) as a fully mesh-less scheme, no grid is necessary; (ii) the computational efforts are directed only to the regions with non-zero vorticity and not to all the domain points as is done in the Eulerian formulations; (iii) the far away downstream boundary condition is taken care automatically which is relevant for the simulation of the flow around a bluff body (or an oscillating body) that has a wide viscous wake.

The two-dimensional aerodynamic characteristics are investigated at a Reynolds number of 1.0×10^5; due to this fact, even with such a high Reynolds number value, no attempt for turbulence modeling were made once these aspects have a strong three-dimensional component; see Alcântara Pereira *et al.* (2002).

2. FORMULATION OF THE PHYSICAL PROBLEM

2.1. Definitions

Figure 1 shows the harmonic in-line motion of the circular cylinder in the uniform fluid flow U=1. The (x, o, y) is the inertial frame of reference and the (ξ, o, η) is the coordinate system fixed to the cylinder. The position and velocity of the local moving coordinate at the center of the circular cylinder are defined, respectively, as

$$\xi = A\sin(\lambda t) \tag{1}$$

$$\dot{\xi} = u_{osc} = A\lambda\cos(\lambda t), \tag{2}$$

where A is the body oscillation amplitude, $\lambda=2\pi f_b$ is the angular velocity and f_b is the body oscillation frequency.

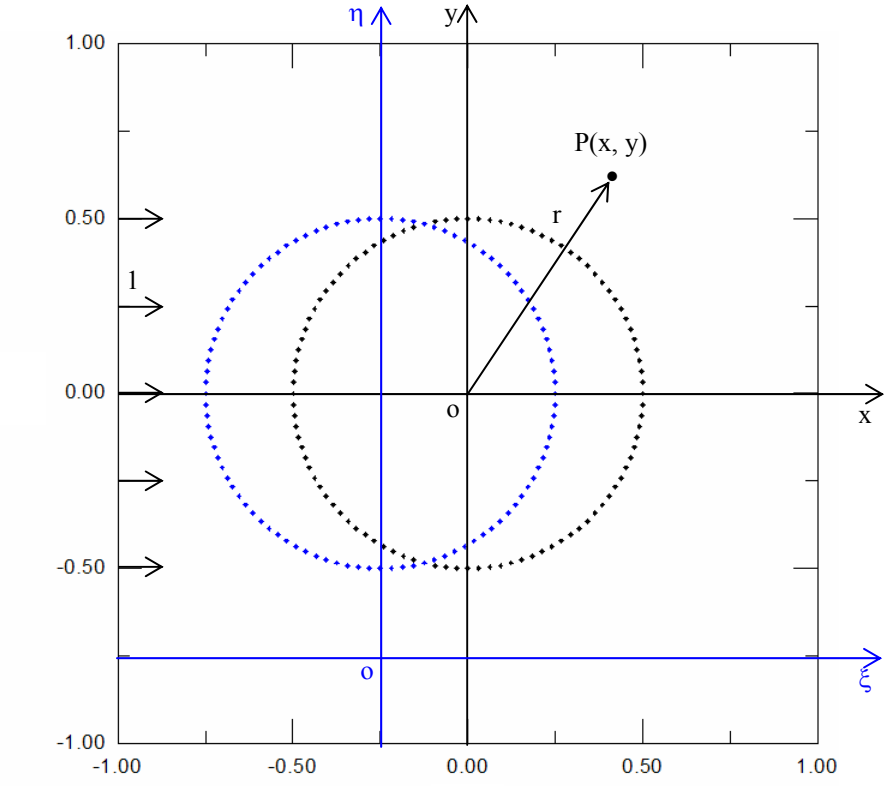

Figure 1 – Definitions

The boundary S of the fluid domain is $S = S_b \cup S_\infty$; being S_∞ the far away boundary, which can be viewed as $r = \sqrt{x^2 + y^2} \to \infty$, and S_b the circular cylinder surface.

2.2. Governing Equations

For an incompressible fluid flow the continuity is written as

$$\nabla \cdot \mathbf{u} = 0 \tag{3}$$

where $\mathbf{u} \equiv (u, v)$ is the velocity vector.

If, in addition, the fluid is Newtonian with constant properties the momentum equation is represented by the Navier-Stokes equation as

$$\frac{\partial \mathbf{u}}{\partial t} + \mathbf{u} \cdot \nabla \mathbf{u} = -\nabla p + \frac{1}{Re} \nabla^2 \mathbf{u} \,. \tag{4}$$

Here, p is the pressure field and Re stands for the Reynolds number defined as $Re = \frac{U\,D}{\upsilon}$, where υ the kinematic viscosity of fluid and D is the diameter cylinder; the dimensionless time is D/U.

On the cylinder surface the adherence condition has to be satisfied. This condition is better specified in terms of the normal and tangential components as

$$(\mathbf{u} \cdot \mathbf{n}) = (\mathbf{v} \cdot \mathbf{n}) \ \text{ on } S_b \text{, the impenetrability condition} \tag{5}$$

$$(\mathbf{u} \cdot \boldsymbol{\tau}) = (\mathbf{v} \cdot \boldsymbol{\tau}) \ \text{ on } S_b \text{, the no-slip condition} \tag{6}$$

where $\mathbf{n}$ and $\boldsymbol{\tau}$ are unit normal and tangential vectors and $\mathbf{v}$ is the body surface velocity vector.

Far from the body (for $r \to \infty$, in Fig. 1) one assumes that the perturbation due to the body motion fades away, that is

$$|\mathbf{u}| \to 1 \,. \tag{7}$$

3. THE VORTEX METHOD

3.1. Viscous Splitting Algorithm (Chorin, 1973)

Taking the curl of the Navier-Stokes equation and with some algebraic manipulations one gets the vorticity equation which presents no pressure term. In two-dimensions this equation reads

$$\frac{\partial \omega}{\partial t} + \mathbf{u} \cdot \nabla \omega = \frac{1}{Re} \nabla^2 \omega \tag{8}$$

where $\omega(\mathbf{x}, t) = \nabla \times \mathbf{u}(\mathbf{x}, t)$ represents the only non-zero component of the vorticity field (observe that the pressure is absent from the formulation).

The left hand side of the above equation carries all the information needed for the convection of vorticity while the right hand side governs the diffusion. Following Chorin (1973) we use the viscous splitting algorithm, which, for the same time step of the numerical simulation, says that

Convection of vorticity is governed by

$$\frac{\partial \omega}{\partial t} + \mathbf{u} \cdot \nabla \omega = 0 \tag{9}$$

Diffusion of vorticity is governed by

$$\frac{\partial \omega}{\partial t} = \frac{1}{Re} \nabla^2 \omega \,. \tag{10}$$

3.2. Convection and diffusion of vorticity

The vortex method proceeds by discretizing spatially the vorticity field using a cloud of elemental vortices, which are characterized by a distribution of vorticity, ς_{σ_i} (commonly called the cutoff function), the circulation strength Γ_i and the core size σ_i. Thus, the discretized vorticity is expressed by

$$\omega(\mathbf{x},t) \approx \omega^h(\mathbf{x},t) = \sum_{i=1}^{Z} \Gamma_i(t)\varsigma_{\sigma_i}(\mathbf{x}-\mathbf{x}_i(t)). \tag{11}$$

where Z is the number of point vortices of the cloud used to simulate the vorticity field.

In this paper, as the diffusion effects are simulated using the random displacement method (Lewis, 1999), we assume that the core sizes are uniform ($\sigma_i = \sigma$), and use the Gaussian distribution as the cut-off function; this choice of the cut-off function leads to the Lamb Vortices (Leonard, 1980); thus

$$\varsigma_\sigma(\mathbf{x}) = \frac{1}{\pi\sigma^2}\exp\left(-\frac{|\mathbf{x}|^2}{\sigma^2}\right). \tag{12}$$

The numerical analysis is conducted over a series of small discrete time steps Δt for each of which a discrete vortex element $\Gamma_{(i)}$ is shed from each impeller surface element. The intensity $\Gamma_{(i)}$ of these newly generated vortices is determined using the no-slip condition, see Eq. (6).

For the convection of the discrete vortices of the cloud, Eq. (9) is written in its Lagrangian form as

$$\frac{dx^{(i)}}{dt} = u^{(i)}(x,y,t) \tag{13}$$

$$\frac{dy^{(i)}}{dt} = v^{(i)}(x,y,t) \tag{14}$$

being (i) = 1, Z.

The convective motion of each vortex generated on the body surface is determined by integration of each vortex path equation, which can be written, using a first order Euler scheme, as

$$x^{(i)}(t+\Delta t) = x^{(i)}(t) + \left[u^{(i)}(t)\right]\Delta t \tag{15}$$

$$y^{(i)}(t+\Delta t) = y^{(i)}(t) + \left[v^{(i)}(t)\right]\Delta t\,. \tag{16}$$

The diffusion of vorticity is taken care of using the random walk method. The random displacement $Z_d \equiv (x_d, y_d)$, with a zero mean and a $(2\Delta t/Re)$ variance, for vortex (i) is defined as

$$x_d^{(i)} = [\cos(2\pi Q)]\sqrt{\frac{4\Delta t}{Re}\ln\left(\frac{1}{P}\right)} \tag{17}$$

$$y_d^{(i)} = [\sin(2\pi Q)]\sqrt{\frac{4\Delta t}{Re}\ln\left(\frac{1}{P}\right)} \tag{18}$$

where P and Q are random numbers in the range 0.0 to 1.0. Therefore the final displacement is written as

$$x^{(i)}(t+\Delta t) = x^{(i)}(t) + \left[u^{(i)}(t)\right]\Delta t + x_d^{(i)} \tag{19}$$

$$y^{(i)}(t+\Delta t) = y^{(i)}(t) + \left[v^{(i)}(t)\right]\Delta t + y_d^{(i)}\,. \tag{20}$$

3.3. Numerical Implementation

The $u^{(i)}$ and $v^{(i)}$ components of the velocity induced at the location of the vortex (i) can be written as

$$u^{(i)} = 1 + ub^{(i)} + uv^{(i)} \tag{21}$$

$$v^{(i)} = 0 + vb^{(i)} + vv^{(i)} \tag{22}$$

where, $\mathbf{ui}^{(i)} \equiv [1, 0]$ is the velocity vector of uniform flow,

$\mathbf{ub}^{(i)} \equiv [ub^{(i)}, vb^{(i)}]$ is the velocity vector induced by the cylinder at the location of vortex (i),

$\mathbf{uv}^{(i)} \equiv [uv^{(i)}, vv^{(i)}]$ is the velocity vector induced at the vortex (i) due to the vortex cloud.

The $\mathbf{ui}^{(i)}$ calculations present no problems. The body contributes with $\mathbf{ub}(\mathbf{x}, t)$, which can be obtained, for example, using the Boundary Element Method (Katz and Plotkin, 1991). The two components can be written as

$$ub^{(i)} = \sum_{k=1}^{NP} \psi_k \, uc_k^{(i)} \tag{23}$$

$$vb^{(i)} = \sum_{k=1}^{NP} \psi_k \, vc_k^{(i)} \tag{24}$$

where NP is the total number of flat source panels representing cylinder surface. It is assumed that the source strength per length is constant such that $\psi_k = \text{const}$ and $uc_k^{(i)}$ and $vc_k^{(i)}$ are the components of the velocity induced at vortex (i) by a unit strength flat source panel located at k.

As the body surface is simulated by NP straight line panels (Panels Method) it is convenient to calculate the body induced velocity in the moving coordinate system. For that one has to observe the following

- The fluid velocity on the body surface is written as

$$\mathbf{u}(\xi, \eta; t) = \left[A \, \lambda \cos(\lambda \, t)\right]\mathbf{i} + 0 \, \mathbf{j} \, . \tag{25}$$

- The velocity induced by the body, according to the Panels Method calculations, is indicated by $[ub(\xi,\eta), vb(\xi,\eta)]$; this is the velocity induced at the vortex (i), located at the point $[\xi(t), \eta(t)]$; thus

$$ub^{(i)}(x, y; t) = ub(\xi, \eta; t) + A \, \lambda \cos(\lambda \, t) \tag{26}$$

$$vb^{(i)}(x, y; t) = vb(\xi, \eta; t) \, . \tag{27}$$

The velocity **uv** is obtained from the vorticity field by means of the Biot-Savart law

$$\mathbf{uv}(\mathbf{x}, t) = \int (\nabla \times \mathbf{G})(\mathbf{x} - \mathbf{x}')\omega(\mathbf{x}', t)d\mathbf{x}' = \int \mathbf{K}(\mathbf{x} - \mathbf{x}')\omega(\mathbf{x}', t)d\mathbf{x}' = (\mathbf{K} * \omega)(\mathbf{x}, t) \tag{28}$$

where $\mathbf{K} = \nabla \times \mathbf{G}$ is the Biot-Savart kernel, **G** is the Green's function for the Poisson equation, and $*$ represents the convolution operation.

Once, with the vorticity field the pressure calculation starts with the Bernoulli function, defined by Uhlman (1992) as

$$\overline{Y} = p + \frac{u^2}{2}, \; u = |\mathbf{u}| \, . \tag{29}$$

Kamemoto (1993) used the same function and starting from the Navier-Stokes equations was able to write a Poisson equation for the pressure. This equation was solved using a finite difference scheme. Here the same Poisson equation was derived and its solution was obtained through the following integral formulation (Shintani and Akamatsu, 1994)

$$H\overline{Y_i} - \int_S \overline{Y}\nabla\Xi_i \cdot \mathbf{e}_n dS = \iint_\Omega \nabla\Xi_i \cdot (\mathbf{u}\times\boldsymbol{\omega}) d\Omega - \frac{1}{Re}\int_S (\nabla\Xi_i \times \boldsymbol{\omega})\cdot \mathbf{e}_n dS \tag{30}$$

where $H = 1$ in the fluid domain, $H = 0.5$ on the boundaries, Ξ is a fundamental solution of the Laplace equation and $\mathbf{e}_n$ is the unit vector normal to the solid surfaces.

The drag and lift coefficients are expressed by

$$C_D = -\sum_{k=1}^{NP} 2(p_k - p_\infty)\Delta S_k \sin\beta_k = -\sum_{k=1}^{NP} C_P \Delta S_k \sin\beta_k \tag{31}$$

$$C_L = -\sum_{k=1}^{NP} 2(p_k - p_\infty)\Delta S_k \cos\beta_k = -\sum_{k=1}^{NP} C_P \Delta S_k \cos\beta_k \tag{32}$$

where ΔS_k is the length and β_k is the angle and both of the k^{th}-panel.

4. RESULTS AND DISCUSSION

We preliminary investigate the flow around a fixed circular cylinder to analyze the consistence of the vortex code and to define some numerical parameters; as for example the number of panels used to define the cylinder surface. For this particular configuration, the cylinder surface was represented by NP=100 flat source panels with constant density. The simulation was performed up to 800 time steps with magnitude Δt=0.05. During each time step the new vortex elements are shedding into the cloud through a displacement $\varepsilon=\sigma_0$=0.0032d normal to the straight-line elements (panels); see Ricci (2002).

Table 1 shows that the numerical results agree very well with the experimental ones obtained by Blevins (1984), which have an uncertainty of about 10%. The results from Mustto *et al*. (1998) were obtained numerically using a slightly different vortex method from the present implementation. The agreement between the two numerical methods is very good for the Strouhal number, and both results are close to the experimental value. The present drag coefficient shows a higher value as compared to the experimental result. One should observe, that the three-dimensional effects are non-negligible for the Reynolds number used in the present simulation ($Re = 1.0\times10^5$). Therefore one can expect that a two-dimensional computation of such a flow must produce higher values for the drag coefficient. On the other hand, the Strouhal number is insensitive to these three-dimensional effects. The mean numerical lift coefficient, although very small, is not zero which is due to numerical approximations. The aerodynamic forces computations were evaluated between t=20 and t=40.

Table 1. Mean drag and lift coefficients and Strouhal number for fixed circular cylinder

$Re = 1.0\times10^5$	$\overline{C_D}$	$\overline{C_L}$	$\overline{St}$
Blevins (1984)	1.20	-	0.19
Mustto *et al.* (1998)	1.22	-	0.22
Present Simulation	1.22	0.07	0.20

The Strouhal number is defined as

$$St = \frac{f\,d}{U} \tag{33}$$

where f is the detachment frequency of vortices of the lift coefficient. One should observe that the lift coefficient oscillates with a dimensionless frequency (Strouhal number) that is one half the frequency of oscillation of the drag coefficient curve. More details of this preliminary study are discussed in Hirata *et al*. (2008).

In this paper, the body Strouhal number is defined as

$$St_b = \frac{f_b\,d}{U}. \tag{34}$$

Table 2 summarize the numerical results, including the mean lift and drag coefficient, Strouhal vortex shedding frequency of the drag coefficient, St_0, for fixed amplitude of A/d = 0.50 and given forcing frequencies.

Table 2. Present numerical results (A/d=0.50 and Re=1.0x10^5)

St_b	$\overline{St_0}$	St_b/St	$\overline{C_D}$	$\overline{C_L}$
0.002	0.421	0.008	1.189	0.036
0.003	0.421	0.016	1.028	0.041
0.008	0.403	0.040	1.147	–0.025
0.016	0.384	0.080	1.368	0.039
0.048	0.049	0.239	1.375	0.260
0.064	0.061	0.318	0.992	–0.102
0.095	0.097	0.477	1.062	0.201
0.111	0.111	0.557	0.779	0.0003
0.127	0.128	0.637	0.478	–0.090
0.143	0.142	0.716	0.201	–0.010
0.159	0.160	0.796	0.117	–0.007
0.191	0.190	0.955	–0.137	–0.0003
0.207	0.206	1.035	–0.190	–0.001
0.239	0.238	1.194	–0.367	–0.002

Figure 2 shows the behavior of drag and lift coefficients for case St_b = 0.016. The lift curve has approximately a dimensionless frequency about twice the frequency of the drag coefficient (St_0). As showed in Fig. 4a, for cylinder oscillations around St_b = 0.016 the mode of vortex formation can be categorized still as fixed cylinder mode.

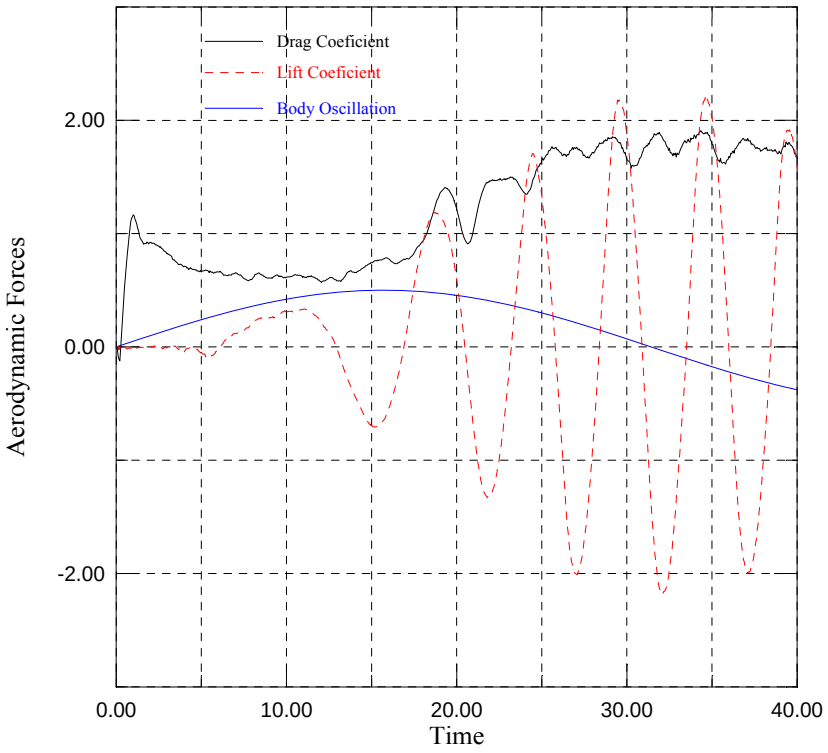

Figure 2. Time history of drag and lift coefficients for A/d = 0.5, St_b = 0.016 and Re=1.0x10^5.

It is seen here that the increase in cylinder vibration is accompanied with the decrease in vortex shedding frequency leading to symmetrical mode of vortex formation, see Fig. 4b. For the symmetrical mode, a pair of vortices is shed in

phase from both sides of the cylinder during one oscillation cycle. Figure 3 shows the time-dependent drag and lift coefficients for oscillating circular cylinder at A/d = 0.5, St_b = 0.239 and Re=1.0x10^5. As soon in Fig. 3 the lift coefficient no oscillates and the frequency of oscillation of the drag coefficient curve is closer to the vortex shedding frequency from the fixed cylinder.

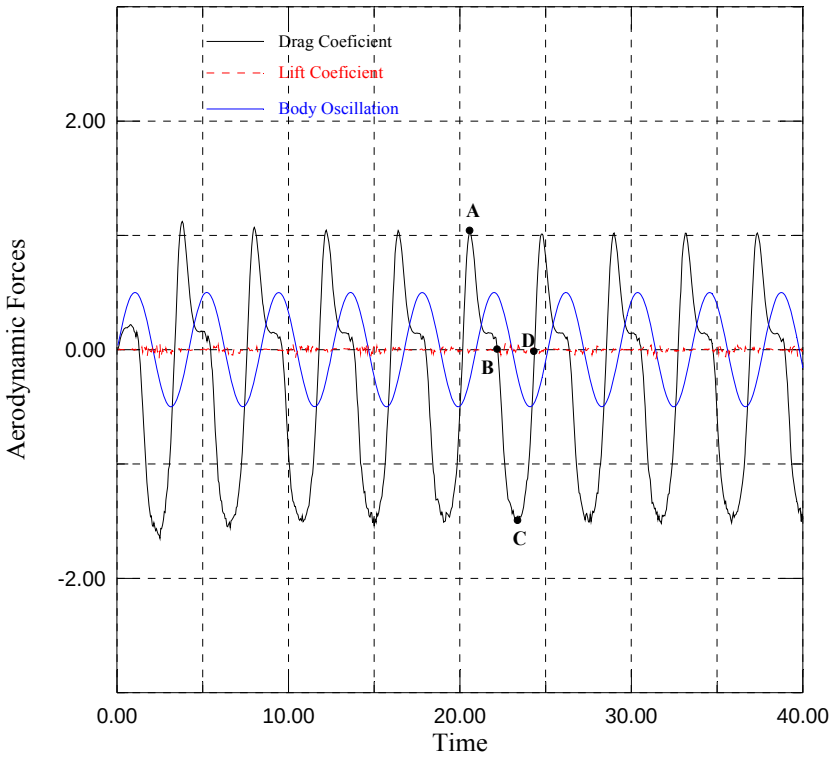

Figure 3. Time history of drag and lift coefficients for A/d = 0.5, St_b = 0.239 and Re=1.0x10^5.

Instant B in Fig. 3 is defined by a maximum value of the cylinder oscillation amplitude; at this moment a pair of vortices is shed in phase from both sides of the cylinder surface and moving toward the viscous wake; this structure is indicated in Fig. 5.

(a) St_b = 0.016

(b) St_b = 0.239

Figure 4. Two different modes of vortex formation for circular cylinder vibration, for A/d = 0.5 and Re=1.0x10^5.

Ongoren and Rockwell (1988) carried out extensive experiments from an in-line oscillating circular cylinder at low Reynolds number Re = 855. Two basic vortex shedding patterns were observed for the forced oscillation for A/d=0.13: one with symmetrical mode and the other with four antisymmetrical modes. According their experiments, in general, the cylinder oscillations are predominantly in the symmetrical mode, while the antisymmetrical modes are induced by the naturally occurring large-scale vortex formation.

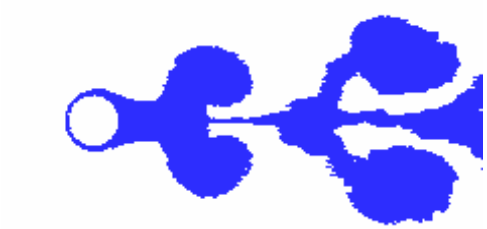

Figure 5. Near wake behavior at an instant represented by point B for in-line oscillation cylinder.

Figure 6 reveal that a small vortex structure is detached from the cylinder and is incorporated into the viscous wake behind a large vortex structure at A/d = 0.5 and St_b = 0.064. This behavior is coherent with those antisymmetrical modes reported Ongoren and Rockwell (1988). The temporal history of the aerodynamics forces is presented in Fig. 7.

Figure 6. Mode of vortex formation for circular cylinder vibration, for A/d = 0.5, St_b = 0.064 and Re=1.0x10^5.

Further analyses are necessary to understand the aerodynamic loads and vortex shedding behavior through different oscillating frequencies and amplitudes.

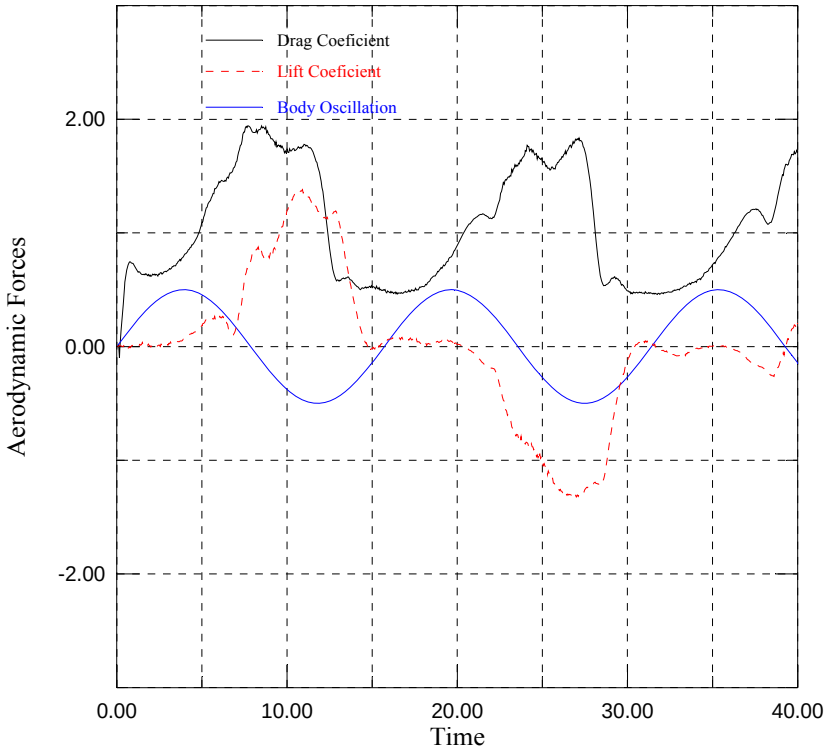

Figure 7. Time history of drag and lift coefficients for A/d = 0.5, St_b = 0.064 and Re=1.0x10^5.

5. CONCLUSIONS

In the present study, we used the vortex method to investigate fluid flows around an in-line oscillating cylinder with a high value of the Reynolds number. The methodology developed in this paper to understand the complex mechanisms of regimes of vortex shedding is greatly simplified by the utilization of the vortex method. In general, when vortices are shed into the wake of a cylindrical body, they cause a periodic lift force on the body at the frequency of shedding and a drag force having twice that frequency. In this work the forced vibration of circular cylinders associated with these aerodynamic forces have been investigated for Reynolds number of around 100,000 and a large amplitude of A/d=0.50.

For the symmetrical mode, our results showed that the vortex shedding synchronized with the cylinder vibration (which is known as the lock-in phenomenon) when the amplitude of lift coefficient is around zero and the vibration frequency around $St_b/St = 1.0$. Finally, despite the differences presented, the results are promising, that encourages performing additional tests in order to explore the phenomena in more details.

6. ACKNOWLEDGEMENTS

This research was supported by the CNPq (Brazilian Research Agency) Proc. 470420/2008-1, FAPERJ (Research Foundation of the State of Rio de Janeiro) Proc. E-26/112/013/2008 and FAPEMIG (Research Foundation of the State of Minas Gerais) Proc. TEC APQ-01074-08.

7. REFERENCES

Alcântara Pereira, L.A., Hirata, M.H. and Manzanares Filho, N., 2004, "Wake and Aerodynamics Loads in Multiple Bodies - Application to Turbomachinery Blade Rows", J. Wind Eng. Ind. Aerodyn., 92, pp. 477-491.

Alcântara Pereira, L.A., Ricci, J.E.R., Hirata, M.H. and Silveira-Neto, A., 2002, "Simulation of Vortex-Shedding Flow about a Circular Cylinder with Turbulence Modeling", Intern'l Society of CFD, Vol. 11, No. 3, October, pp. 315-322.

Bearman, P.W., 1984, "Vortex Shedding from Oscillating Bluff Bodies", Annu. Rev. Fluid Mech., 16:195-222.

Blevins, R.D., 1990, "Flow Induced Vibrations", New York, Van Nostrand Reinhold.

Blevins, R. D., 1984, Applied Fluid Dynamics Handbook, Van Nostrand Reinhold, Co.

Chorin, A.J., 1973, "Numerical Study of Slightly Viscous Flow", Journal of Fluid Mechanics, Vol. 57, pp. 785-796.

Griffin, O.M. and Hall, M.S., 1991, "Review-Vortex Shedding Lock-On and Flow Control in Bluff Body Wakes", Journal of Fluids Engineering, Vol. 113, pp. 526-537.

Hirata, M. H., Alcântara Pereira, L. A., Recicar, J. N., Moura, W. H., 2008, "High Reynolds Number Oscillations of a Circular Cylinder", J. of the Braz. Soc. Of Mech. Sci. & Eng., Vol. XXX, No. 4, pp. 300-308.

Kamemoto, K., 2004, "On Contribution of Advanced Vortex Element Methods Toward Virtual Reality of Unsteady Vortical Flows in the New Generation of CFD", Proceedings of the 10th Brazilian Congress of Thermal Sciences and Engineering-ENCIT 2004, Rio de Janeiro, Brazil, Nov. 29 - Dec. 03, Invited Lecture-CIT04-IL04.

Kamemoto, K., 1993, "Procedure to Estimate Unstead Pressure Distribution for Vortex Method" (In Japanese), Trans. Jpn. Soc. Mech. Eng., Vol. 59, No. 568 B, pp. 3708-3713.

Katz, J. and Plotkin, A., 1991, "Low Speed Aerodynamics: From Wing Theory to Panel Methods". McGraw Hill, Inc.

Koopman, G.H., 1967, "The Vortex Wakes of Vibrating Cylinders at Low Reynolds Numbers", Journal of Fluid Mechanics, Vol. 28, pp. 501-518.

Leonard, A., 1980, "Vortex Methods for Flow Simulation", J. Comput. Phys., Vol. 37, pp. 289-335.

Lewis, R.I., 1999, "Vortex Element Methods, the Most Natural Approach to Flow Simulation - A Review of Methodology with Applications", Proceedings of 1st Int. Conference on Vortex Methods, Kobe, Nov. 4-5, pp. 1-15.

Mustto, A. A., Hirata, M. H. and Bodstein, G. C. R., 1998, "Discrete Vortex Method Simulation of the Flow Around a Circular Cylinder with and without Rotation", A.I.A.A. Paper 98-2409, Proceedings of the 16th A.I.A.A. Applied Aerodynamics Conference, Albuquerque, NM, USA, June.

Ongoren, A. and Rockwell, D., 1988, "Flow Structure from an Oscillating Cylinder. Part 2: Mode competition in the near Wake", Journal of Fluid Mechanics, 191: 225-245.

Ricci, J.E.R., 2002, "Numerical Simulation of the Flow around a Body in the Vicinity of a Plane Using Vortex Method", Ph.D. Thesis, Mechanical Engineering Institute, UNIFEI, Itajubá, MG, Brazil (in Portuguese).

Sarpkaya, T., 1989, "Computational Methods with Vortices - The 1988 Freeman Scholar Lecture", Journal of Fluids Engineering, Vol. 111, pp. 5-52.

Sarpkaya, T., 1979, "Vortex-Induced Oscillations", ASME J. Appl. Mech., 46:241-258.

Sethian, J.I., 1991, "A Brief Overview of Vortex Method, Vortex Methods and Vortex Motion", SIAM. Philadelphia, pp. 1-32.

Shintani, M. and Akamatsu, T, 1994, "Investigation of Two Dimensional Discrete Vortex Method with Viscous Diffusion Model", Computational Fluid Dynamics Journal, Vol. 3, No. 2, pp. 237-254.

Stock, M.J., 2007, "Summary of Vortex Methods Literature (A lifting document rife with opinion)", April, 18: © 2002-2007 Mark J. Stock.

Uhlman, J.S., 1992, "An Integral Equation Formulation of the Equation of an Incompressible Fluid", Naval Undersea Warfare Center, T.R. 10-086.

Williamson, C.H.K. and Govardhan, R., 2004, "Vortex Induced Vibrations", Annu. Rev. Fluid Mech., 36:413-455.

8. RESPONSIBILITY NOTICE

The author(s) is (are) the only responsible for the printed material included in this paper.